Immunizations on small worlds of tree-based wireless sensor networks

Li Qiao(李 峤)[a)†], Zhang Bai-Hai(张百海)[a)], Cui Ling-Guo(崔灵果)[a)],
Fan Zhun(范 衡)[b)], and Athanasios V. Vasilakos[c)]

[a)] *School of Automation, Beijing Institute of Technology, Beijing* 100081, *China*

[b)] *Department of Mechanical Engineering, Technical University of Denmark,* 2800 *Kgs. Lyngby, Denmark*

[c)] *Department of Computer and Telecommunications Engineering, University of Western Macedonia, Kozani, Greece*

(Received 27 October 2011; revised manuscript received 18 November 2011)

The sensor virus is a serious threat, as an attacker can simply send a single packet to compromise the entire sensor network. Epidemics become drastic with link additions among sensors when the small world phenomena occur. Two immunization strategies, uniform immunization and temporary immunization, are conducted on small worlds of tree-based wireless sensor networks to combat the sensor viruses. With the former strategy, the infection extends exponentially, although the immunization effectively reduces the contagion speed. With the latter strategy, recurrent contagion oscillations occur in the small world when the spatial–temporal dynamics of the epidemic are considered. The oscillations come from the small-world structure and the temporary immunization. Mathematical analyses on the small world of the Cayley tree are presented to reveal the epidemic dynamics with the two immunization strategies.

Keywords: epidemic, immunization, small world, tree-based networks

PACS: 02.50.–r, 05.50.+q, 05.65.+b **DOI:** 10.1088/1674-1056/21/5/050205

1. Introduction

Recent years have seen the deployment of wireless sensor networks (WSNs) in a variety of applications, including habitat and environmental monitoring,[1] precision agriculture, security surveillance,[2] etc. Sensors are being deployed in more and more efficient ways. Tree topology is a kind of architecture that is frequently used, and is ubiquitous in the deployment of wireless sensor nodes. Some routing protocols, topology control algorithms, and aggregation schedules of wireless sensor networks are helpful for constructing tree-based networks.

The DQT (distributed quad-tree) is an in-network tree framework, which achieves distance sensitivity and resiliency for event-based querying, and greatly reduces the cost of complex range querying.[3] The HAA (hybrid address assignment scheme) uses a tree address structure to make the proposed scheme less susceptible to the physical distribution of the WSN devices.[4] The SCT (semantic/spatial correlation-aware tree) has a simple, scalable, and distributed tree structure that addresses the practical challenges in the context of aggregations in the WSNs.[5] With this structure, the total cost of the aggregation tree can be minimized. The LEMA (localized energy-efficient multicast algorithm) uses a function to locally estimate the energy-efficient paths to multiple the destinations.[6] It is able to deal with the inherent errors of the WSNs. Several tree-based protocols based on MST (minimal spanning tree)[7] have also attracted much attention recently. The BCDCP (base-station controlled dynamic clustering protocol) introduces an MST to connect cluster heads and adopts an iterative cluster splitting algorithm to choose cluster heads or form clusters.[8] It distributes energy dissipation evenly among all sensor nodes to improve the network lifetime and average energy saving. The CTPEDCA (cluster-based and tree-based power efficient data collection and aggregation protocol for WSNs) is based on a clustering and MST routing strategy for cluster heads, which uses the MST to improve the transmission routing mechanism among the cluster heads so that only one cluster head communicates directly with the faraway base station in each round.[9] Most tree-based protocols use multi-hop tree topologies, which are famous for energy saving in data gathering and transferring.

Compared with the regular computer systems, it is even easier for the sensors to be compromised by

†Corresponding author. E-mail: liqq007@gmail.com

virus attacks. Sensor nodes in the same network are homogeneous in both hardware and software. They do not have complicated hardware architectures or operating systems to protect against attacks due to cost and resource constraints. In this research, we only consider viruses like sensor worms. If a sensor worm attacks a network, the epidemic propagates rapidly from one side to another. Yang *et al.* studied the worm propagation in a wireless sensor network and considered the propagation as a random process in a random network.[10] De *et al.* investigated the potential disastrous threat of node compromise spreading in a wireless sensor network.[11] They focused on the possible epidemic breakout based on a random network. In routing protocols, topology control algorithms and aggregation schedules, the random graphs cannot completely indicate the structure characteristics of wireless sensor networks. In tree-based networks, random link additions among nodes occur inevitably for the use of omnidirectional antennae. Obstacles, adjustments of radio energy, joins of new members, and errors of location precision all incur link additions. In this paper, small-world phenomena[12] existing in the tree-based wireless sensor networks are studied. Due to the shortcuts in small worlds, the epidemic propagation becomes more drastic in the network. The immunization is one of the most common strategies for combating the outbreak of sensor viruses. The epidemic dynamics and the immunization strategies are analyzed in the small world of the tree-based wireless sensor network.

The small-world phenomena were first investigated in sociology, where individuals were often linked by a short chain of acquaintances. Duncan proposed an alternative model for the small-world phenomena by using the graph theory.[13] Recent research has shown that the small-world phenomena are ubiquitous in nature, society, and technology. Small worlds are also observed in wireless networks.[14,15] Some researches have been conducting studies on the dynamics of epidemic propagations on small-world networks.[16−18] Developing strategies for controlling the dynamics of epidemics as they spread through complex population networks is now a field of great concern.[19−23] Stone *et al.* studied the relative effects of vaccinations and avoidances of infected individuals in a susceptible–infected–recovered (SIR) epidemic model on a dynamic small-world network.[23] Da Gama and Nunes studied the effect of the network structure on the immune models for life diseases and found that in addition to the reduction of the effective transmission rate, spatial correlations might strongly enhance the stochastic fluctuation.[24] Stone and Livak–Hinenzon analyzed the recurrent oscillations occurring in the small-world networks.[25] Li *et al.* studied the short message spreadings in complex networks.[26] Song and Jiang proposed an epidemic-spreading model for networks with nodes of different anti-attack abilities and edges of nonuniform transmission.[27] The success of an infectious disease to invade a population is strongly dependent on the population's specific connectivity structure.

Our research focuses on the immunization strategies for combating epidemic propagations on small worlds of tree-base wireless sensor networks. The uniform immunization procedure, which consists of the random distribution of immune individuals, is conducted in the small world. The infection extends exponentially although the uniform immunization effectively reduces the propagation speed. If we consider the spatiotemporal state of the epidemic and conduct the temporary immunization on the small world, oscillation waves are found in the network. Oscillations come from the small-world structure and the temporary immunization.

The rest of the paper is organized as follows. Our small-world model and the basic ideas are described in Section 2. Two immunization strategies and the mathematical analyses are presented in Section 3. Numerical simulations are presented in Section 4. The paper is concluded in Section 5.

2. Small-world model

We consider a two-dimensional network composed of N nodes. All nodes are symmetric with similar properties, including range of radio coverage, energy of battery, etc. The nodes are randomly distributed in the network. The small-world model proposed in this paper starts with the regular tree abstract, the Cayley tree, and link additions are then added to construct a small-world network. In the Cayley tree, each node has K nearest neighbors, $K \geq 2$. There are $N-1$ links between the nodes in the Cayley tree. If p is defined as the average number of shortcuts per bond (link) on the underlying tree, there are $p(N-1)$ link additions and $(p+1)(N-1)$ links altogether in the small world. The proposed abstract neglects the actual distance information, which simplifies the problem and represents a spatial graph model. Figure 1 shows small worlds of tree-based networks and our proposed small-world model. In the figures, the circles denote nodes

in the wireless sensor network, the rectangle denotes the base station collecting data from the network, the black lines denote bonds, and the dashed lines denote link additions in the small worlds. The actual distance information is neglected, and the bonds only describe logical links in the small world. The small world of a SCT[5] is shown in Fig. 1(a). The small world of a MST[7] is shown in Fig. 1(b). The Cayley tree with link additions is shown in Fig. 1(c), in which each node has three nearest neighbors, $K = 3$. The following mathematical analyses of two immunization strategies are presented on the Cayley tree with link additions, which reveals the two immunization processes for combating epidemic propagations.

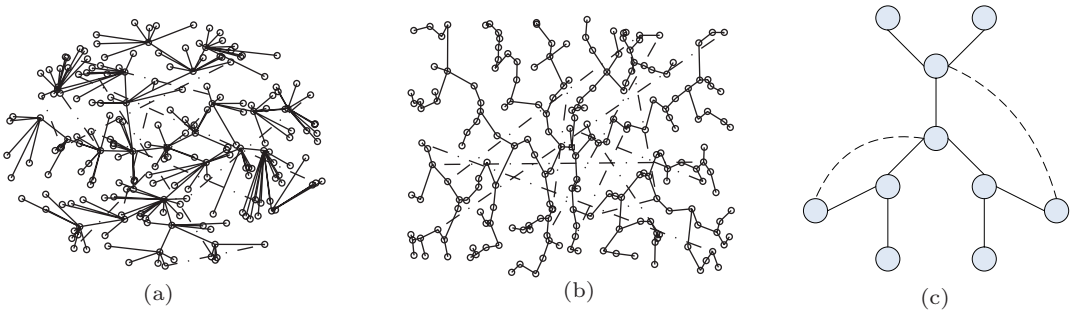

Fig. 1. Small worlds of (a) SCT, (b) MST, and (c) the Cayley tree with link additions.

Traditionally, networks of complex topologies have been described with the random graph theory and the regular graph theory. The random graph is used for depicting the network topology in the random graph theory, in which two nodes are connected with a random probability. If all nodes are randomly movable or they flood messages under no rule, then the random graph is suitable for depicting the network topology. The mean-field theory is used to analyze the virus propagations on the random network.[10] The network has a fixed deployment structure in the regular graph theory. The virus propagation on the regular topology is a standard percolation problem.[28] Our proposed small-world abstract has a hierarchical tree-based structure with random connections occurring between nodes, which describes the complex dynamics of the wireless sensor networks. If some nodes are movable, and most nodes are unmovable in the network, random connections occur in the hierarchical topology. The small-world abstract describes the hybrid structure perfectly. As we have analyzed, obstacles, adjustments of radio energy, joins of new members, and errors of location precision all incur in the small world. The small-world phenomenon is one basic characteristic of the wireless networks.

3. Immunization strategies

In network G, $S(t)$, $I(t)$, and $R(t)$ are the nodes in the states of susceptible (S), infectious (I), and immune/recovered (R) at time t, respectively. We know that $S(t) + I(t) + R(t) = N$. Let S_t, I_t, and R_t be the proportions of susceptible, infective, and recovered nodes in the network at time t, respectively, we have $S_t + I_t + R_t = 1$. We can partition the infected nodes in the network into $I(t_0), I(t_1), I(t_2), \ldots$ at time $t_0, t_1, t_2, \ldots$, respectively. With the uniform immunization, $I(t+1)$ contains more nodes than $I(t)$ if the infected nodes attack their neighbors in each time unit. The $I(t)$ increases rapidly with time t as the epidemic spreads on the network, although the immunization reduces the propagation speed. With the temporary immunization, $I(t)$ increases or decreases periodically with time t if the ratio of the infectious period τ_{I} to the immune period τ_{R} is suitable. Shortcuts are uniformly added besides the inherent edges in the original tree topology with the average degree $\langle k \rangle = (1+p)K$. If node i is susceptible, and it has k_i neighbors, of which k_{inf} are infected. Then, node i will become infected with probability k_{inf}/k_i. It is noted that i will become infected with probability 1 if all its neighbors are infected. Besides this parameter-free mechanism, there may be other reasonable choices. For example, if the susceptible has a probability h of contagion with each infected neighbor, its probability of infection becomes $[1-(1-h)^{k_{\mathrm{inf}}}]$.

3.1. Uniform immunization

We now analyze the epidemiological process with the uniform immunization, which is used frequently in

homogeneous small-world networks. We assume that there is only one infected node in the initial stage, ρ is defined as the fraction of immune nodes present in the network, and the remaining nodes are susceptible (healthy). The immune nodes cannot become infected or transmit the infection to their neighbors. The infected nodes only attack their nearest susceptible neighbors in each time unit. During the propagation, the understratum plays a key role and is an essential factor considered in the immunization strategies. Two sources contribute to the number of infected nodes, one is the susceptible neighbor nodes on the underlying topology, and the other is the susceptible nodes reachable via the shortcuts.

Following the above description, $I(t)$ can be calculated by

$$I(t) = \sum_{t'=0}^{t} (1-\rho)ha(t')[1 + 2\xi^{-1} I(t-t')], \qquad (1)$$

where $a(t')$ is the number of attacked neighbors on the underlying topology, h is the infection probability, and ξ is the average distance between the ends of shortcuts, $\xi = \frac{N}{(N-1)p}$. For mathematical analyses of epidemics on the small world, three cases are considered. If $a(t')$ is a constant C_K, the epidemiological process is considered, and

$$I(t) = \sum_{t'=0}^{t} (1-\rho)hC_K \left[1 + 2p\frac{N-1}{N} I(t-t')\right]. \qquad (2)$$

The sum can be approximated by an integral

$$\begin{aligned} I(t) &= \int_0^t (1-\rho)hC_K \left[1 + 2p\frac{N-1}{N} I(t-t')\right] \mathrm{d}t' \\ &= (1-\rho)hC_K t + \frac{2p(1-\rho)hC_K(N-1)}{N} \\ &\quad \times \int_0^t I(t')\,\mathrm{d}t'. \end{aligned} \qquad (3)$$

The first-order derivative with respect to t can be obtained as

$$\frac{\mathrm{d}I(t)}{\mathrm{d}t} = (1-\rho)hC_K + \frac{2p(1-\rho)hC_K(N-1)}{N} I(t), \qquad (4)$$

and the solution is obtained as

$$\begin{aligned} I(t) &= \left[1 + \frac{N}{2p(N-1)}\right] \mathrm{e}^{\frac{2p(1-\rho)hC_K(N-1)t}{N}} \\ &\quad - \frac{N}{2p(N-1)}. \end{aligned} \qquad (5)$$

With $N \to \infty$,

$$I(t) = \left(1 + \frac{1}{2p}\right) \mathrm{e}^{2p(1-\rho)hC_K t} - \frac{1}{2p}. \qquad (6)$$

We can see that the number of infected nodes increases exponentially with t, and the result coincides with that on the ring topology.[13] When $I(t) = N$, all nodes are infected, we obtain the threshold

$$t_c \approx \frac{N}{2p(1-\rho)hC_K(N-1)} \ln \frac{2pN(N-1)+N}{2p(N-1)+N}.$$

In fact, $a(t')$ has more complex mathematical forms when the viruses spread on the underlying topology. If $a(t') = C_K t'$, $I(t)$ can be calculated as

$$\begin{aligned} I(t) &= \sum_{t'=0}^{t} (1-\rho)hC_K t' \left[1 + 2p\frac{N-1}{N} I(t-t')\right] \\ &= \int_0^t (1-\rho)hC_K t' \left[1 + 2p\frac{N-1}{N} I(t-t')\right] \mathrm{d}t' \\ &= (1-\rho)hC_K \int_0^t t'\,\mathrm{d}t' \\ &\quad + \frac{2p(1-\rho)hC_K(N-1)}{N} t \int_0^t I(t')\,\mathrm{d}t' \\ &\quad - \frac{2p(1-\rho)hC_K(N-1)}{N} \int_0^t t' I(t')\,\mathrm{d}t'. \end{aligned} \qquad (7)$$

Both sides are differentiated with respect to t, we obtain

$$\begin{aligned} \frac{\mathrm{d}I(t)}{\mathrm{d}t} &= (1-\rho)hC_K t + \frac{2p(1-\rho)hC_K(N-1)}{N} \\ &\quad \times \int_0^t I(t')\,\mathrm{d}t'. \end{aligned} \qquad (8)$$

The second-order derivative with respect to t can be obtained as

$$\begin{aligned} \frac{\mathrm{d}^2 I(t)}{\mathrm{d}t^2} &= (1-\rho)hC_K \\ &\quad + \frac{2p(1-\rho)hC_K(N-1)}{N} I(t). \end{aligned} \qquad (9)$$

It is a second-order linear differential equation, and can be solved as

$$\begin{aligned} I(t) &= C_1 \mathrm{e}^{\sqrt{\frac{2p(1-\rho)hC_K(N-1)}{N}}t} \\ &\quad + C_2 \mathrm{e}^{-\sqrt{\frac{2p(1-\rho)hC_K(N-1)}{N}}t} - \frac{N}{2p(N-1)}, \end{aligned} \qquad (10)$$

where C_1 and C_2 are two constants. There is only one infected node in the network at $t = 0$, i.e., $C_1 + C_2 = 1 + \frac{N}{2p(N-1)}$.
With $N \to \infty$,

$$\begin{aligned} I(t) &= C_1 \mathrm{e}^{\sqrt{2p(1-\rho)hC_K}t} \\ &\quad + C_2 \mathrm{e}^{-\sqrt{2p(1-\rho)hC_K}t} - \frac{1}{2p}, \end{aligned} \qquad (11)$$

and $C_1 + C_2 = 1 + \frac{1}{2p}$.

The infected parent node may attack all its children nodes in each time unit, $a(t') = C_K(K-1)^{t'}$, then

$$\begin{aligned} I(t) &= \sum_{t'=0}^{t}(1-\rho)hC_K(K-1)^{t'} \\ &\quad\times\left[1+2p\frac{N-1}{N}I(t-t')\right] \\ &= \int_0^t(1-\rho)hC_K(K-1)^{t'} \\ &\quad\times\left[1+2p\frac{N-1}{N}I(t-t')\right]\mathrm{d}t' \\ &= (1-\rho)hC_K\int_0^t(K-1)^{t'}\,\mathrm{d}t' \\ &\quad+\frac{2p(1-\rho)hC_K(N-1)}{N}(K-1)^t \\ &\quad\times\int_0^t(K-1)^{-t'}I(t')\mathrm{d}t'. \end{aligned} \tag{12}$$

Let $F(t) = (K-1)^t\int_0^t(K-1)^{-t'}I(t')\mathrm{d}t'$, and differentiate both sides with respect to t, we obtain

$$F'(t) = \ln(K-1)\cdot F(t) + I(t). \tag{13}$$

From Eq. (12), we can rewrite $I(t)$ as

$$\begin{aligned} I(t) &= (1-\rho)hC_K\int_0^t(K-1)^{t'}\,\mathrm{d}t' \\ &\quad+\frac{2p(1-\rho)hC_K(N-1)}{N}F(t). \end{aligned} \tag{14}$$

Then,

$$\begin{aligned} F(t) &= \frac{N}{2p(1-\rho)hC_K(N-1)}I(t) \\ &\quad-\frac{N}{2p(N-1)}\int_0^t(K-1)^{t'}\,\mathrm{d}t'. \end{aligned} \tag{15}$$

Differentiate both sides with respect to t, we have

$$\begin{aligned} F'(t) &= \frac{N}{2p(1-\rho)hC_K(N-1)}I'(t) \\ &\quad-\frac{N}{2p(N-1)}(K-1)^t. \end{aligned} \tag{16}$$

From Eqs. (13), (15), and (16), we obtain

$$\begin{aligned} &I'(t) - (1-\rho)hC_K(K-1)^t \\ &= \ln(K-1)\left[I(t) - (1-\rho)hC_K\int_0^t(K-1)^{t'}\,\mathrm{d}t'\right] \\ &\quad+\frac{2p(1-\rho)hC_K(N-1)}{N}I(t). \end{aligned} \tag{17}$$

The second-order derivative with respect to t can be obtained as

$$I''(t) = \left[\ln(K-1) + \frac{2p(1-\rho)hC_K(N-1)}{N}\right]I'(t). \tag{18}$$

It can be solved as

$$\begin{aligned} I(t) &= C_3\exp\left(\left[\ln(K-1)\right.\right. \\ &\quad\left.\left.+\frac{2p(1-\rho)hC_K(N-1)}{N}\right]t\right) + C_4, \end{aligned} \tag{19}$$

where C_3 and C_4 are two constants. At $t=0$, there are C_K infected nodes in the network, i.e., $C_3 + C_4 = C_K$.
With $N\to\infty$,

$$I(t) = C_3\,\mathrm{e}^{[\ln(K-1)+2p(1-\rho)hC_K]t} + C_4, \tag{20}$$

and $C_3 + C_4 = C_K$.

The uniform immunization is equivalent to the removal of individuals from the relevant population. It reduces the effective average number of neighbors per node and slows down the propagation. From the above analyses, we can see that although different epidemiological processes occur on the underlying tree topology, the total number of infected nodes increases exponentially with the uniform immunization. The presence of the immunization will effectively reduce the prevalence speed by a factor $(1-\rho)$.

3.2. Temporary immunization

The success of the epidemic to invade a network is strongly dependent on the network's specific connectivity structure. We are interested in a further theoretical understanding of the spatial–temporal dynamics of the epidemic on the small world of tree-based networks. A period of temporary immunization is conducted on the node after it is infected, which is then removed after an intrinsic time delay. As a result, recurrent propagation oscillations of infection occur in the network. The epidemic cycles arise because of the delayed susceptible–infectious–recovered–susceptible (SIRS)[24] process. In the SIRS process, the susceptible nodes become infected, recover with the temporary immunization, but return to the susceptible state when the immunization wears off.

The state of the node at the (i,j)-th location of the lattice, $x_{ij}(t)$, can be S, I, or R. The following rules guide the state transitions:

$$x_{i,j}(t) \in \mathrm{S} \to \begin{cases} x_{i,j}(t+1) \in \mathrm{I}, & \text{with probability } 1-(1-h)^{k_{\mathrm{inf}}^{i,j}(t)}(t), \\ x_{i,j}(t+1) \in \mathrm{S}, & \text{otherwise}, \end{cases} \tag{21}$$

$$x_{i,j}(t_0) \in \mathrm{I} \to x_{i,j}(t_0+1) \in \mathrm{I} \to \cdots \to x_{i,j}(t_0+\tau_{\mathrm{I}}) \in \mathrm{R} \to x_{i,j}(t_0+\tau_{\mathrm{I}}+1) \in \mathrm{R} \to \cdots \to x_{i,j}(t_0+\tau_0) \in \mathrm{S}, \tag{22}$$

where h is the infection probability, $k_{\mathrm{inf}}^{i,j}(t)$ is the total number of infectious contacts of the node at time t, t_0 is the initial time, τ_{I} is the time period that a node remains infectious, and τ_{R} is the period that a node remains immune. We assume that $\tau_{\mathrm{I}} = 1$, the proportion of recovered nodes can be described by the sum $\sum_{i=1}^{\tau_0-1} I_{t-i}$, and S_t can be calculated as

$$S_t = 1 - I_t - \sum_{i=1}^{\tau_0-1} I_{t-i}, \tag{23}$$

where $\tau_0 = \tau_{\mathrm{I}} + \tau_{\mathrm{R}}$. For the homogeneous small-world abstract, the number of infected neighbors of each node is the sum of the number of neighbors on the underlying topology and that of the nodes connected with shortcuts, which at time t are I_tK and I_tpK, respectively.

Let h_K be the probability that such a node is infected by a neighbor in a given time step. Let h_p be the probability that such a node is infected by a node connected with the shortcut. Then the spread of the epidemic can be described with the following model of the SIRS dynamics:

$$\begin{aligned} I_{t+1} &= [1-(1-h_K)^{I_tK}(1-h_p)^{I_tpK}]S_t \\ &= [1-(1-h_{\mathrm{eff}})^{I_tK}]S_t, \end{aligned} \tag{24}$$

where h_{eff} is defined as

$$1 - h_{\mathrm{eff}} = (1-h_K)(1-h_p)^p. \tag{25}$$

Equation (24) captures both the time delay dynamics resulting from the temporary immunization of the infection and the effects of the shortcuts. The recurrent propagation oscillations relay on the infection, the recovery, and the reinfection of the nodes in the small world. The shortcuts of the small world and the temporary immunization each play an important role in this procedure.

4. Simulations

Simulations of epidemic propagations with immunizations on small worlds are presented in this section. We study the time evolutions of the infected numbers in small worlds of SCT and MST by using a large number of experiments assuming that there is a portion of nodes infected in the initial stage. We assume that node i is susceptible, and it has k_i neighbors, of which k_{inf} are infected. Then, node i will become infected with probability k_{inf}/k_i. The network is conducted with the uniform immunization or the temporary immunization. The epidemiological behaviors with the immunizations are studied when the small-world phenomena occur. The propagations based on mathematical analyses are also presented in this section. The simulations show that the mathematical analyses reveal the dynamic characteristics of the epidemic propagations with the two immunization strategies.

4.1. Simulations of the uniform immunization

Epidemiological behaviors with the uniform immunization are studied when the small-world phenomena occur in the tree-based networks. Figures 2(a) and 2(b) show the time evolutions of the infected numbers with the uniform immunization on small worlds of the

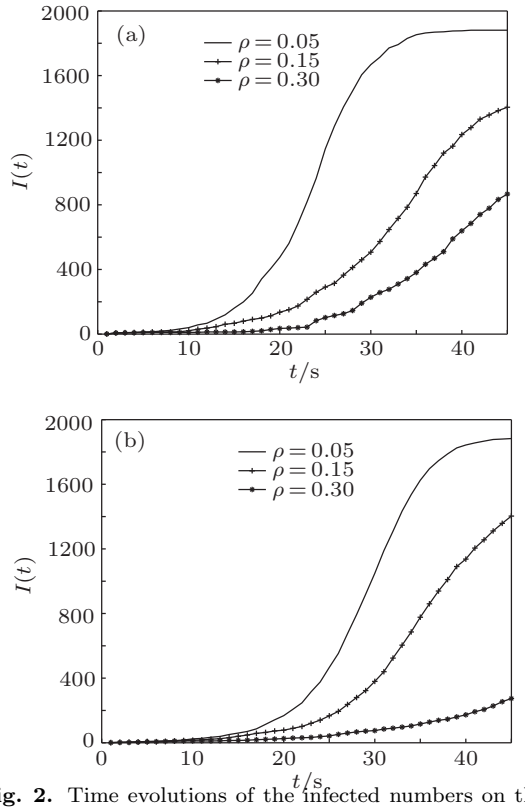

Fig. 2. Time evolutions of the infected numbers on the small worlds of (a) the SCT and (b) the MST with $p = 0.3$ and $N = 2000$.

SCT and the MST, respectively. There is only one infected node in the initial stage. The parameters from Refs. [5] and [7] are used in Fig. 2. The epidemics spread exponentially with the uniform immunization in most time on the two small worlds. In the late stage, the exponential evolution process experiences a decline due to the reduction of the remaining susceptible nodes in the network. The infected number keeps increasing until all nodes are infected in the network. The simulations show that the larger the immunization factor ρ is, the slower the speed of prevalence is. The uniform immunization reduces the effective average number of neighbors for each node and slows down the propagation.

The following simulations depict the epidemiological propagations with the uniform immunization on the small world of the Cayley tree based on the mathematical analyses. For $a(t') = C_K$, a certain number of nodes are attacked on the tree-based topology in each time unit. Due to the shortcuts, the infection extends exponentially with t, as shown in Eq. (5). The duration of each time unit is 10 seconds. Figure 3(a) shows the time evolution of the infected number in the epidemiological process. From the figure, we can see that the speed of the infection decreases as ρ increases. At $t = 43$ s, the infected number in the network is 950 for $\rho = 0.05$, 511 for $\rho = 0.15$, and 201 for $\rho = 0.3$.

For $a(t') = C_K t'$, C_1 and C_2 can be approximately calculated at $t = 0$ s and $t = 10$ s. The duration of each time unit is 10 seconds. Figure 3(b) shows the time evolution of the infected number in the epidemiological process. At $t = 53$ s, the infected number in the network is 924 for $\rho = 0.05$, 657 for $\rho = 0.15$, and 377 for $\rho = 0.3$.

For $a(t') = C_K(K-1)^{t'}$, C_3 and C_4 can be approximately calculated at $t = 0$ s and $t = 10$ s. The duration of each time unit is 10 seconds. Figure 3(c) shows the time evolution of the infected number in the epidemiological process. At $t = 32$ s, the infected number in the network is 778 for $\rho = 0.05$, 520 for $\rho = 0.15$, and 279 for $\rho = 0.3$.

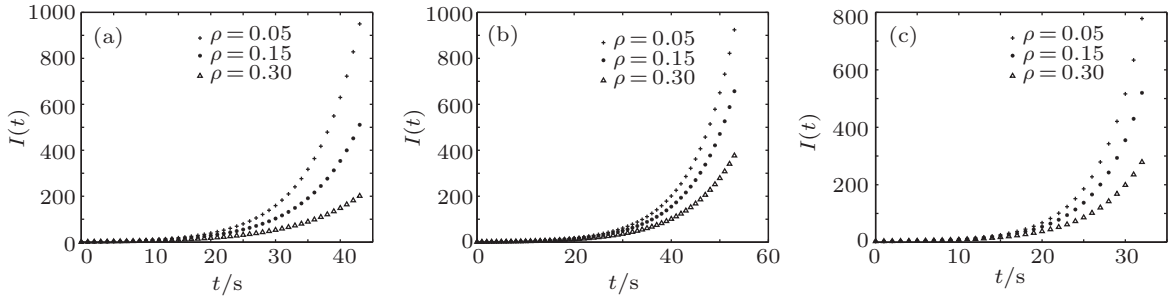

Fig. 3. Epidemiological propagations on the small world of the Cayley tree with $p = 0.3$, $h = 0.8$, $C_K = 3$, $K = 3$, and $N = 1000$. The time evolutions of the infected number are shown for (a) $a(t') = C_K$, (b) $a(t') = C_K t'$, and (c) $a(t') = C_K(K-1)^{t'}$.

Table 1. Infected numbers with the uniform immunization.

$a(t')$ \ ρ	0.05	0.1	0.15	0.2	0.25	0.3	0.35	0.4	0.45
C_K	160	129	103	83	66	53	43	34	27
$C_K t'$	61	56	50	45	40	36	32	28	25
$C_K(K-1)^{t'}$	518	430	356	294	242	199	163	133	108

Table 1 shows the numbers of infected nodes at $t = 30$ s with $p = 0.3$, $h = 0.8$, $C_K = 3$, $K = 3$, and $N = \infty$ for different ρ. Although the uniform immunization reduces the prevalence speed, the total number of infected nodes increases exponentially. The larger the immunization factor ρ is, the slower the speed of the prevalence is.

4.2. Simulations of the temporary immunization

The epidemiological behaviors of sensor worms with the temporary immunization are investigated in the following simulations. Figures 4(a) and 4(b) show the time evolutions of the infected numbers with the temporary immunization on small worlds of the SCT and the MST, respectively. The parameters from

Refs. [5] and [7] are used in Fig. 4. The recurrent waves are observed both spatially and temporally. The periodicity of the wave comes from the small-world structure and the temporary immunization, the reinfection of the recovered nodes after a certain time delay introduced by the temporary immunization in the SIRS procedure.

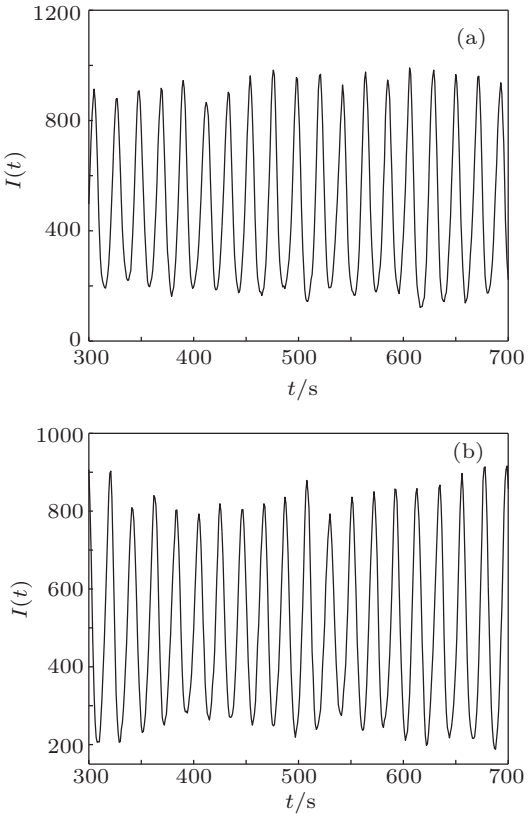

Fig. 4. Time evolutions of the infected numbers on the small worlds of (a) the SCT and (b) the MST with $p = 0.9$ and $N = 2000$.

Figure 5 depicts the recurrent oscillations of the spatio–temporal epidemiological behaviors on the small world of the Cayley tree based on Eq. (24). In the simulations, 2000 nodes are distributed randomly in the network, and 10% nodes are infected in the initial stage. A certain number of neighbors ($K = 4$) are connected directly with each node on the tree-based topology, and pK shortcuts link it with the other ones with $p = 0.4$. The spread of the prevalence is affected by the infection probabilities $h_K = 0.35$ and $h_p = 0.12$. In Fig. 5(a), $\tau_{\rm I} = 1$ and $\tau_{\rm R} = 8$, while in Fig. 5(b), $\tau_{\rm I} = 1$ and $\tau_{\rm R} = 6$. The simulations lead to a better understanding of the epidemic spread with the temporary immunization. The infection probabilities h_K, h_p and the average number p of the shortcuts per bond have great influences on generating the long-term cycles. The periodicity of the waves is the outcome of both the small-world structure and the temporary immunization. The reinfection at the center of the wave after a certain amount of time is due to the shortcuts and the intrinsic time delay introduced by the temporary immunization. On the other hand, the ratio of time period $\tau_{\rm I}$ to time period $\tau_{\rm R}$ has a great influence on generating the long-term cycles. In Fig. 5(b), the number of infected nodes remains a constant after $t = 260$ s. It is the outcome of both the small-world structure and the temporary immunization. An equilibrium is reached between the reinfection and the infection due to the intrinsic time delay introduced by the temporary immunization. The periodic waves based on the mathematical analyses coincide with the recurrent propagation oscillations of epidemics in the small worlds of the SCT and the MST.

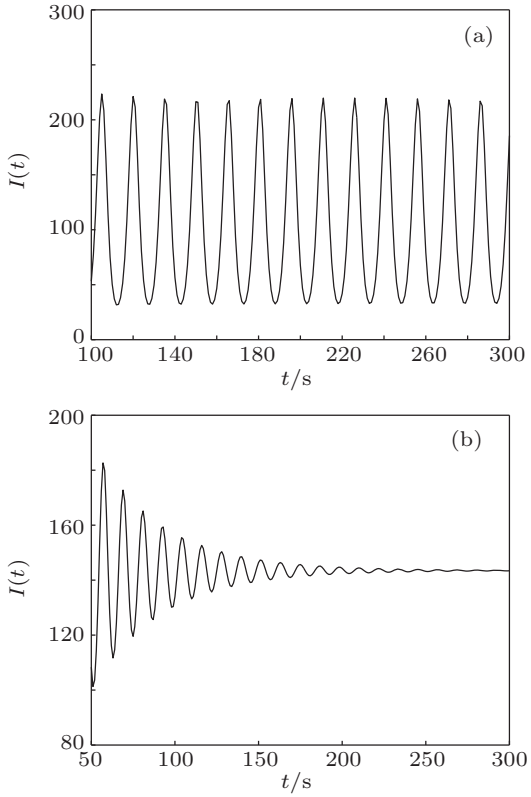

Fig. 5. Epidemiological propagations with the temporary immunization on the small world of the Cayley tree. The time evolutions of the infected number are shown on the small world of the Cayley tree for (a) $\tau_{\rm I} = 1$ and $\tau_{\rm R} = 8$ and (b) $\tau_{\rm I} = 1$ and $\tau_{\rm R} = 6$.

5. Conclusion

Compared with the regular computer systems, it is even easier for the sensors to be compromised by virus attacks. The sensor worm propagates rapidly from one side of the wireless sensor network to another side. Due to the link additions, the small-world phenomena occur, and the epidemic propagation becomes more drastic. Developing strategies to control the dynamics of epidemics as they spread is now a field of

great concern. Two immunization strategies, the uniform immunization and the temporary immunization, are conducted on small worlds of tree-based wireless sensor networks to combat the sensor viruses. Detailed mathematical analyses are presented to reveal the epidemic propagations with the two immunization strategies. With the uniform immunization, which consists of the random distribution of immune individuals, the infection increases exponentially although the immunization effectively reduces the propagation speed. With the temporary immunization, recurrent contagion oscillations occur in the small world when the spatial–temporal dynamics of epidemics are concerned. The oscillations come from the small-world structure and the temporary immunization.

References

[1] Alippi C, Camplani R, Galperti C and Roveri M 2011 *IEEE Sensors J.* **11** 45

[2] Wang X, Wang S and Bi D W 2009 *IEEE Trans. Syst. Man Cybern.* B **39** 1134

[3] Demirbas M, Lu X M and Singla P 2009 *IEEE Trans. Parallel Distrib. Syst.* **20** 1202

[4] Wong Y C, Wang J T, Chang N H, Liu H H and Tseng C C 2008 *IEEE Commun. Lett.* **12** 414

[5] Zhu Y J, Vedantham R, Park S J and Sivakumar R 2008 *Inf. Fusion* **9** 354

[6] Sanchez J A and Ruiz P M 2009 *Wireless Commun. Mobile Comput.* **9** 395

[7] Shen H 1999 *Acta Inform.* **36** 405

[8] Muruganathan S D, Ma D C F, Bhasin R I and Fapojuwo A O 2005 *IEEE Commun. Mag.* **43** S8

[9] Wang W, Wang B W, Liu Z, Guo L J and Xiong W 2011 *Inf. Technol. J.* **10** 557

[10] Yang Y, Zhu S C and Cao G H 2008 *Proceedings of the 9th ACM International Symposium on Mobile Ad Hoc Networking and Computing*, May 26–30, 2008 Hong Kong, China, p. 149

[11] De P, Liu Y and Das S K 2006 *2006 International Symposium on a World of Wireless, Mobile and Multimedia Networks,* June 26–29, 2006 Piscataway, United States, p. 237

[12] Stanley M 1967 *Psychology Today* **2** 60

[13] Duncan J W 1999 *Small Worlds, the Dynamics of Networks between Order and Randomness* (Princeton: Princeton University Press)

[14] Helmy A 2003 *IEEE Commun. Lett.* **7** 490

[15] Li Q, Cui L G, Zhang B H and Fan Z 2010 *Proceedings of the 29th Chinese Control Conference,* July 29–31, 2010 Beijing, China, p. 4677

[16] Moore C and Newman M E J 2000 *Phys. Rev.* E **61** 5678

[17] Huang C Y and Tsai Y S 2010 *Phys.* A *Stat. Mech. Appl.* **389** 604

[18] Walker D M, Allingham D, Lee H W J and Small M 2010 *Phys.* A *Stat. Mech. Appl.* **389** 540

[19] Kuperman M and Abramson G 2001 *Phys. Rev. Lett.* **86** 2909

[20] Keeling M J and Eames K T D 2005 *J. R. Soc. Interface* **2** 295

[21] Olinky R, Huppert A and Stone L 2008 *J. Math. Biol.* **56** 827

[22] Yu X L, Wang X Y, Zhang D M, Liang F and Wu X 2008 *Phys.* A *Stat. Mech. Appl.* **387** 1421

[23] Stone T E, Jones M M and Mckey S R 2010 *Phys.* A *Stat. Mech. Appl.* **389** 5515

[24] Da Gama M M T and Nunes A 2006 *Eur. Phys. J.* B **50** 205

[25] Stone L and Livak-Hinenzon A 2009 *J. R. Soc. Interface* **6** 749

[26] Li M J, Wu Y, Liu W Q and Xiao J H 2009 *Acta Phys. Sin.* **58** 5251 (in Chinese)

[27] Song Y R and Jiang G P 2010 *Acta Phys. Sin.* **59** 7546 (in Chinese)

[28] Dietrich S and Ammon A 1992 *Introduction to Percolation Theory* (London: Burgess Science Press)